Published by :
http://www.ijert.org

International Journal of Engineering Research & Technology (IJERT)
ISSN: 2278-0181
Vol. 12 Issue 07, July-2023

Effects of General Asymmetries on Heavy Vehicles Vertical Displacement Dynamics Responses

Josua K Junias
Department of Mechanical and Metallurgical Engineering, University of Namibia (UNAM)
Ongwediva, Namibia

Fillemon N Nangolo
School of Mechanical, Industrial and Electrical Engineering
Namibia University of Science and Technology (NUST)
Windhoek, Namibia

Petrina T Johannes
Department of Civil and Mining Engineering
University of Namibia
Ongwediva, Namibia

Abstract - The impact of unbalanced heavy vehicle loading on their dynamic responses has led to the need for further investigation into the vertical displacement dynamic response of asymmetrically loaded heavy vehicles. Similarly, the effect of eccentric kinematic excitation on these vehicles also requires attention. Previous studies have focused solely on the effects of either road profiles or asymmetric loading configurations on heavy vehicle dynamic responses, but not on the combined effects of both asymmetrical loading configurations and eccentric kinematic excitation. This study examines the vertical dynamic responses of 3D (24 DOF) models, which are validated and influenced by general asymmetries. Among a population of 225 possible symmetrical and asymmetrical cases of heavy vehicle kinematic excitation and loading configurations, 27 SIMWISE 4D models were selected for analysis. Results indicate that different load distribution on the sprung mass affects the position of the center of mass, thereby influencing the heavy vehicle's dynamic response. Furthermore, the nature of the sprung mass vertical displacement dynamic response is influenced by the eccentric kinematic excitation on the vehicle wheels.

Keywords—asymmetries; excitation; heavy vehicles; translation

I. INTRODUCTION

The effect of asymmetrical loading and cross wind to study models were considered in most revised literatures wherein assumptions had been made that pavements are uniform with no irregularities [1]. The combined general asymmetries due to translating vehicle loading and pavement distress factors are investigated in this study to develop an understanding on transport system vibration responses. Thus, this study intents to extend the preceding vehicle vibration analysis by introducing a model cable of predicting reasonable vertical dynamic response in the presence of general asymmetric loading and asymmetric kinematic excitations. This was achieved by investigating the effects of general asymmetries on vertical vibration of heavy vehicles sprung mass at varying heavy vehicles speed and pavement distress factors geometry (pothole depth) for the similar loading configurations.

In this study, the car-body and chassis component masses were considered to be rigid bodies with all wheel's profiles identical and with no rotational motion. Further, no longitudinal and lateral dynamic response of the system was considered and only the linear characteristics of the springs and dampers of the suspension system were considered. Among other commercial computer simulation packages available for dynamic analysis, only SIMWISE 4D simulation packages was used to analyze the vehicle vertical dynamic response as well as the imposed forces.

II. REVISED LITERATURE

Today's technology made it simple to virtually model complex system either as a sprung mass or unsprung mass. This is worth noting as, even though there exist different vehicle models of several complexities and Degree of Freedom (DOF) that are meant to simulate the vehicles dynamics. They all falls under the two main categories as per approach used to model the system namely; (a) multi-body models that consider the detailed individual rigid bodies that connect with one another kinetically or dynamically to form a detailed assembly equivalent to the entire vehicle system while the (b) lumped-mass vehicle models only consider different parts of the vehicle to be lumped masses, as of an example, the vehicle bodies and wheel sets [2]. It is to be known that the lumped-mass vehicle model was used in simulating the vertical transferred forces due to dynamics of the heavy vehicle due to general eccentricities. In addition to that, for the analysis of the interaction between the vehicle and the road system, the vehicle can be modelled as a 1-dimensional, 2-dimensional or 3-dimensional model.

The vehicle models could be as simple as the single (1) DOF quarter-car models or as complex as Multiple DOF systems models. Models that permit dynamic coupling between a numbers of lumped masses on a study model could be as simplified as 2 DOF mass-damper spring vehicle models as modelled in most studies including that of [3]. Quarter-car models mathematical models has been the accepted as the fundamental mean of validating vibration studies. They are applied in several research works models, whereby, on 2 DOF systems, pavement deterioration post effects (potholes and

International Journal of Engineering Research & Technology (IJERT)
ISSN: 2278-0181
Vol. 12 Issue 07, July-2023

random road profile unevenness) onto mechanical systems mathematical formulations for vibration studies has been applied. They are used to analyze the most assumed symmetrical kinematic excitations on the vehicle wheels as indicated in [3] and several other revised literatures.

Mathematically, a more comparable study was conducted in [4], wherein a 4DOF half car- suspension system is used to verify the effectiveness of half car passive suspension system. Therein, the half car motion defined by the heave movements of the front and rear axle, pitch and heave motion of the unsprung mass of the vehicle was modelled, simulated and controlled using Simulink. In their literature, a mathematical linear passive half car model was presented, as indicated in equation (1) to (4), from which the vertical and rotational body displacement was simulated and investigated.

$$M_1\ddot{x}_1 - C_1[\dot{X}_3 - \dot{X}_1 + a\dot{\theta}] - K_3[X_3 - X_1 + a\theta] + K_1[X_1 - U_1] = 0 \quad (1)$$

$$M_2\ddot{x}_2 - C_2[\dot{X}_3 - \dot{X}_2 - b\dot{\theta}] - K_4[X_3 - X_2 - b\theta] + K_2[X_2 - U_2] = 0 \quad (2)$$

$$M_3\ddot{x}_3 + C_1[\dot{X}_3 - \dot{X}_1 + a\dot{\theta}] + K_3[X_3 - X_1 + a\theta] + C_2[\dot{X}_3 - \dot{X}_2 + b\dot{\theta}] + K_4[X_3 - X_2 - b\theta] = 0 \quad (3)$$

$$J\ddot{\theta} + C_1a[\dot{X}_3 - \dot{X}_1 + a\dot{\theta}] + K_3a[X_3 - X_1 + a\theta] + C_2b[\dot{X}_3 - \dot{X}_2 - b\dot{\theta}] - K_4b[X_3 - X_2 - b\theta] = 0 \quad (4)$$

These multiple DOF system equation of motion can also be defined, as indicated in [4] studies on a 7 DOF damped mechanical system modal parameters, by considering the kinetic energy, potential energy as well as the Rayleigh dissipation function of the system, obtaining the final equation by using the Lagrange equations.

$$\mathbf{M_h}\ddot{q}_j(t) + \mathbf{M_b}\dot{q}j(t) + \mathbf{M_k}q_j(t) = \mathbf{Q_j}(q_j, q_j, t) \quad (5)$$

Where, M_h – is the mass matrix with diagonal element ($\bar{\alpha_{ii}}$) in case of symmetric distribution of the sprung mass, otherwise, the mass matrix is not diagonal – in case of asymmetric distribution of the sprung mass ($\bar{\alpha_{ij}}$), for $i \neq j$. M_b – damping matrix ($\bar{b}_{ij}$), M_k – stiffness matrix ($\bar{a_{ij}}$) and $\boldsymbol{Q}_j$ represents the excitations displacement vectors. Coupled natural frequencies for the bogies and wagon can be obtained from these motion equations by supposing that, during equilibrium, there is no velocity, excitation forces, thus reducing the equation to the form:

$$\mathbf{M_h}\ddot{q}_j(t) + \mathbf{M_k}q_j(t) = [0] \quad (6)$$

From these motion equations, the mode shapes and natural frequencies can be obtained to quantify the simulation model response.

MDOF models have been applied in several vehicle vibration studies. Based on experimental data, a 9 DOF railway wagon asymmetrically loaded in the presence of asymmetric kinematic excitation was developed and validated using the experimental data in [5]. Their findings highlighted the need to develop and utilize models to understand these systems' responses under the influence of various general asymmetries. Various cases of asymmetry including kinematic excitation of the system with three degrees of freedom were developed to solve vertical displacements of the center of gravity and rotations to central axes wherein the elastic support of the plate is combined with parallel viscous dumper [6]. Due to the distribution of sprung mass, the center of mass might shift according to truck bed loading descriptions. With motives to narrow the research scope, several comprehensive three-dimensional vehicles models have been developed in the past, incorporating a full or half of the car-body, two bogies and two wheel-sets in [5] and [7]. These models developed are significant as the full car body model was used to develop the models for this research work.

Early attempts at modelling leaf springs utilized the simple approach based on equivalent springs to represent the vertical and longitudinal force-displacement characteristics of the leaf spring [8]. Reference [8] simplified equivalent mechanical springs model for the elliptic leaf spring that can be incorporated in virtual 3D models to mechanically represent the suspension system of the simplified modelled vehicles were established. These kinds of suspension springs were employed in this study models to ensure the realistic motion response of the leaf spring in addition to its load carrying capabilities while ensuring the stability of these models. The potholes have become more frequent as road infrastructures age [9]. Several other researchers including [3], has conducted studies on wheel-pothole interactions, wherein a fundamental understanding on potholes modelling could be obtained. Their models can be used in the evaluation of vehicle behaviors. Geometrically, a small pothole is defined as being 25mm deep and 200mm wide, the medium pothole as 25 to 50mm deep and 500mm wide. The large potholes are those with a depth greater than 50mm deep and 500mm width [10].

III. MODEL DEFINITION

In SIMWISE 4D, the three-axle tandem drive heavy vehicle was designed with the cabin, chassis, and loading platform combined into a single unit onto which payloads are loaded in different ways, also connected to the chassis. The leaf springs, as defined by reference [8], link the unsprung mass to the sprung mass, while the wheels, which are modeled as linear springs, connect the tandem beam to the pavement sections. Figures 1 and 2 illustrate this design.

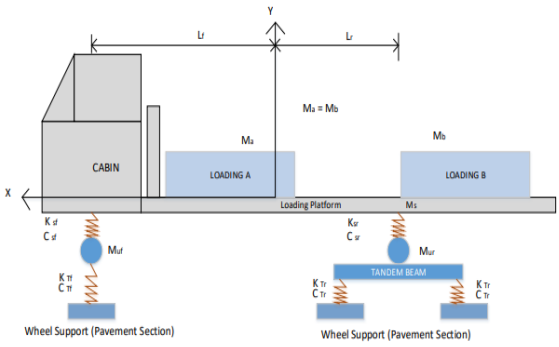

Figure 1: 18 DOF Heavy Vehicle Pavement model (longitudinal axes)

The distance Lf and Lr are used to determine the center of mass (COM) of a heavy vehicle in relation to its front and rear axle. This allows for an equal distribution of weight throughout the vehicle.

International Journal of Engineering Research & Technology (IJERT)
ISSN: 2278-0181
Vol. 12 Issue 07, July-2023

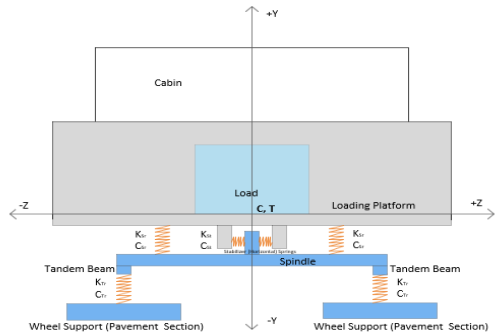

Figure 2: 18 DOF Heavy Vehicle Pavement model

(Transverse axes)

The simulation properties of the suspension system in the figures above were defined using the simulation parameters listed in Table 2, which were obtained from [15]. The two loadings placed on the loading platform are represented by Ma and Mb, which indicate their masses.

Table 1: Simulation Model Parameters

Parameters Description	Parameter
Mass of the Truck (m_s)	7200.0 kg
Truck Pitch moment of inertia (I)	100000.0 kgm^2
Front tire and axle assembly mass (m_{uf})	353.0 kg
Rear tire and axle assembly mass (m_{ur})	653.0 kg
Front axle suspension stiffness (K_{sf})	295.3 kN/m
Rear axle suspension stiffness (K_{sr})	797.3 kN/m
Front axle suspension damping coefficient (C_{sf})	2.9 kNs/m
Rear axle suspension damping coefficient (C_{sr})	5.9 kNs/m
Front tire suspension stiffness (K_{Tf})	1100.0 kN/m
Rear tire suspension stiffness (K_{Tr})	2200.0 kN/m
Front tire suspension damping coefficient (C_{Tf})	0.4 kNs/m
Rear tire suspension damping coefficient (C_{Tr})	0.8 kNs/m
Distance from front axle to Center of Gravity (l_f)	3.757 m
Distance from rear axle to Center of Gravity (l_r)	2.441 m

In this article, the general differences that will be discussed are based on two models: loading configuration and kinematic excitation. The heavy vehicle will be traveling at speeds of 60km/h and 80km/h over potholes with depths of 25mm and 50mm. The symmetric loading configuration (A) involves placing the payloads evenly on the loading bed with their longitudinal central axes collinear to the loading bed's central axes. The symmetrical kinematic excitation (I) involves exciting all the wheels simultaneously. Asymmetric loading configurations were also sampled, with configuration (B) involving placing all the payloads parallel to the longest edge of the loading bed and configuration (E) involving placing all the payloads towards one of the back corners of the loading bed. Sampled asymmetric kinematic excitations were also defined, with excitation (III) involving exciting both rear axle wheels at the same time and excitation (V) involving exciting only the front left wheel of the front axle and the back left wheel of the rear axle at the same time. These models were sampled to show the effects of asymmetrical excitations on the wheel system and asymmetrical loadings on the system. Other possible general asymmetrical cases are listed in Table 1.

Table 2:Models Loading Configuration Versus Kinematic Excitations

Loading Configuration \ Excitation Configuration		I	II	III	IV	V
A		AI	AII	AIII	AIV	AV
B		B I	B II	B III	B IV	B V
C		C I	C II	C III	C IV	C V
D		D I	D II	D III	D IV	D V
E		E I	E II	E III	E IV	E V

The functions presented in Table 2 define three different groups of kinematic excitations that are sampled, depending on the speed of the heavy vehicle and the degree of pavement distress (indicated by pothole depth).

Table 2: Categorized Kinematic Excitation Forcing Functions

Excitation	Excitation Function
$\omega_{25,\,60}$	If(and(time>11.3 s, time<12.1 s), (25*Sin(2.4*time)), 0)
$\omega_{25,\,80}$	If(and(time>11.0 s, time<11.6 s), (25*Sin(3.2*time)), 0)
$\omega_{50,\,60}$	If(and(time>12.7 s, time<14.0 s), (50*Sin(1.2*time)), 0)

In this scenario, the term, $\omega_{r,V}$ denotes the speed at which the wheel appears to come into contact with the pavement when encountering a pothole, just before hitting the opposite end of the pothole. This speed is determined by dividing the heavy vehicle's speed by the depth of the pothole (measured in millimeters) and is represented by r, with v indicating the truck's speed in kilometers per hour. This method is used to replicate the effects of wheels encountering potholes at various speeds. These responses consider the speed at which the suspension pushes the wheel downward to create contact with the ground. The responses use a time-restricted sine wave function, with peak-to-trough amplitudes of 25 mm and 50 mm, to impose kinematic excitations on the unsprung mass and the sprung mass, whose data were examined.

IV. RESULTS AND DISCUSSION

To analyze the proposed general asymmetrical cases and gain insight into the pavement-vehicle interaction, a 24DOF (degrees of freedom) model was created for simulation to extract data for analytical solutions. The effects of general asymmetries on the shifting of the center of mass (COM) were then examined, followed by an analysis of the dynamic responses of the control model's vertical displacement. The results of this analysis will be compared to those of other models. The COM was monitored

International Journal of Engineering Research & Technology (IJERT)
ISSN: 2278-0181
Vol. 12 Issue 07, July-2023

at various time instants when the models were in a state of static equilibrium and dynamic motion had ceased, with the values recorded in Table 3.

Table 3: Chassis Static Equilibrium Position (COM)

Loading Configuration	X (mm)	Y (mm)	Z (mm)
A	-0.198	-24.1	0.00148
B	-0.208	-24.2	5.19
E	-0.775	-23.4	2.59

Table 4 shows the static equilibrium positions of the sprung mass (chassis) and the extent to which the center of mass (COM) has shifted away from the origin due to the distribution of self-weight among the lumped masses. The downward shift in the COM of both models is likely due to the weight of the payload and the self-weight of the vehicle's lumped masses. The symmetrical loading configuration resulted in a vertical displacement of the COM of 24.1 mm from the pre-defined origin (0, 0, 0) mm. Notably, the COM of the E loading configuration was slightly lower on the y-axis than that of the B loading configuration, by 2.49%, and 2.90% lower than the control factor loading configuration (A), with a downward shift of 23.4 mm. The E loading configuration also showed a high COM shift along the longitudinal x-axis, compared to the other two loading configurations, likely due to the overall mass distribution of the lumped masses. The eccentric weight distribution on the chassis caused the COM to shift along the transverse z-axis and the longitudinal x-axis, as seen in the B and E loading configurations. The load distribution, which was eccentric toward the long edge of the loading platform, caused a 5.19mm shift in the COM along the transverse axis compared to the COM shifts of the control model and 50% more than the E load-configured heavy vehicle chassis. Additionally, the orientation of the vehicle models modeled in Table 4 supports these findings.

Table 4: Chassis Static Equilibrium Orientation

Loading Configuration	Rx (Deg)	Ry (Deg)	Rz (Deg)
A	-0.0015	0.000185	0.0216
B	0.969	0.00268	0.0226
E	0.484	0.00173	0.0862

Other loading configurations, such as B and E, appear to have a significant orientation about the longitudinal axis compared to the control loading factor A, which has an insignificant orientation. This is most likely due to the distribution of payloads on the loading platform towards the back corners of the vehicle, causing a slight decrease in the vertical and longitudinal COM, but a significant orientation of the chassis along the transverse principal axis. Both loading configurations showed insignificant orientations about the vertical axis. The B loading configuration resulted in higher orientations about the longitudinal axis compared to the control loading factor A.

In terms of dynamic response, the vertical displacement dynamic responses of the control model (AIw25-60) were observed in Figure 3, where the effect of wheel-pothole interactions could be seen between 11.3 seconds and 12.1 seconds. The heavy vehicle chassis exhibited moderate amplitude harmonic motion for about 5 seconds as it decayed to its static equilibrium position after the wheels interacted with the potholes, indicating an underdamped system with a high damping ratio.

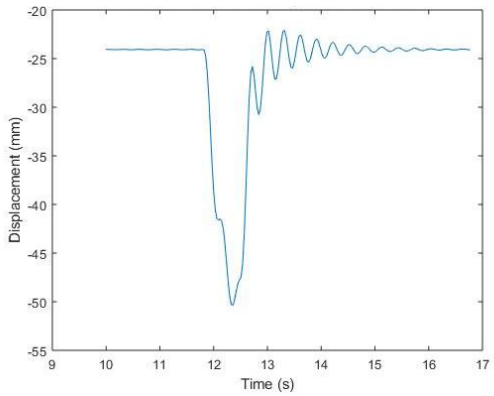

Figure 3: Control Model COM Vertical Dynamic response

When a 25 mm pothole is encountered by both wheels, the sprung mass experiences a rapid downward motion, which is counteracted by the upward acceleration of the unsprung mass as the wheels impact the opposite end of the pothole. This results in a high amplitude dynamic response during the wheel-pothole interaction period.

Frequency analysis of the response, as shown in Figure 4, revealed three significant frequency signals at 5.1 Hz, 7.7 Hz, and 11.9 Hz. These frequencies likely represent the significant vertical dynamic responses of the rear, sprung mass, and front axles, respectively, after the heavy vehicle has encountered potholes on the pavement. The large dynamic vertical displacements of the axles and sprung mass contribute more to these responses than their orientations about the transverse or lateral axes.

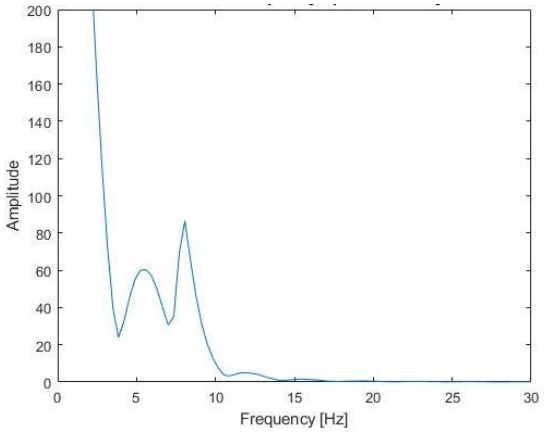

Figure 4: Control Model Frequency Spectrum Analysis

According to the frequency spectrum analysis in Figure 4, the dominant frequency of the vertical displacement dynamic response of the sprung mass is about 7.7 Hz. This can be explained by the fact that the system is symmetrically loaded and excited on both wheels, which minimizes the influence of lateral and longitudinal dynamic responses and their orientations. The

International Journal of Engineering Research & Technology (IJERT)
ISSN: 2278-0181
Vol. 12 Issue 07, July-2023

low signal response at a frequency of 11.9 Hz suggests a low vertical dynamic response of the front axle, possibly due to the front wheels' high stiffness and elastic properties and low mass concentration. On the other hand, load distribution towards the back of the vehicle leads to high signal rear axle vertical displacement response amplitudes of about 60 mm at a frequency of 5.1 Hz.

Figures 5 and 6 display a comparison between the vertical displacement dynamic responses of the control model and the asymmetrical models when driving at a speed of 60 km/h over a pothole with a depth of 25 mm.

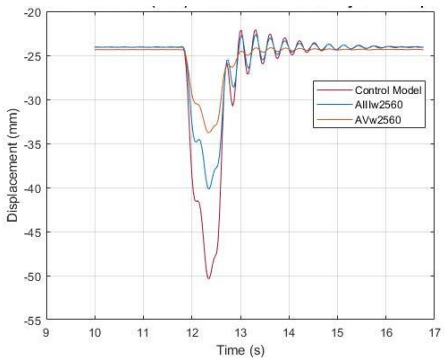

Figure 5: Control Model Versus A(III and V) W25-60 Models Sprung Mass Vertical Dynamic Response (Time Domain)

Although there are notable variations in the amplitude of the sprung mass vertical dynamic responses due to the different kinematic excitations applied to the wheels, Figure 5 demonstrates that the dynamic responses of the sprung mass exhibit similar inertial effects in the time domain. The amplitudes of the models' vertical dynamic responses are amplified by the kinematic excitations, which are influenced by inertia, as shown in the frequency domain analysis results in Figure 6. The control model exhibited the highest signal amplitude, with the V kinematically excited models showing the least signal amplitude at similar frequencies.

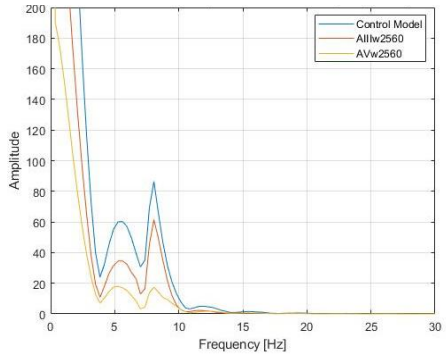

Figure 6: Control Model Versus A(III and V) W25-60 Models Sprung Mass Vertical Dynamic Response (Frequency Spectrum Analysis)

The reason for this is that when both wheels encounter a pothole simultaneously, the resulting motion only causes the sprung mass to move vertically downwards, accelerating it in the same direction. However, the V kinematic excitation does not have a significant effect on the vertical displacement of the sprung mass COM, resulting in lower amplitudes observed at similar frequencies.

The researchers also performed a similar analysis on all other load configurations using the same kinematic excitation but with varying vehicle speeds and pothole depths. For instance, they investigated the case of a vehicle moving at 80 km/h over a 25 mm pothole depth. In this scenario, they observed a similar type of sprung mass vertical dynamic response with relatively high amplitudes compared to the control model's (AIw25-60) vertical displacement dynamic response of the sprung mass.

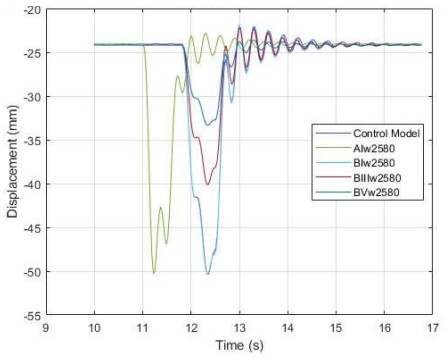

Figure 7: Control Model Versus AIw25-80 Versus B(I, III and V)W25-80 Models Sprung Mass Vertical Dynamic Response (Time Domain)

Figure 7 illustrates the sprung mass vertical displacement dynamic time domain response of the control model, AIw25-80, and B(I, III, V)w25-80 models. It can be observed that the B load configured models exhibit significantly higher dynamic response amplitudes compared to the A load configured models, except for the control model. Additionally, the V kinematic excitation leads to a lower downward shift of the sprung mass COM compared to the symmetrical I kinematic excitation on the same model. The higher displacement dynamic response amplitude of the B load configured models could be attributed to the inertia effects of the sprung mass resulting from the post effects of kinematic excitations amplified by the eccentric distribution of the load over the suspension system. This is because one side of the suspension system is dynamically and compressively loaded, while the other side is under tensile loading.

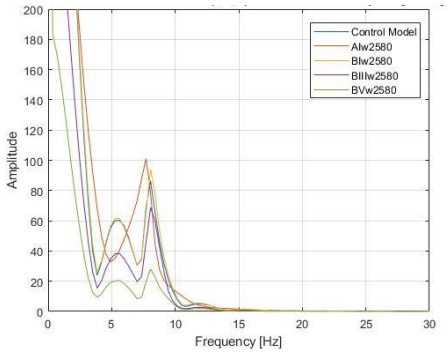

Figure 8: Control Model Versus AIw25-80Versus B(I, III and V) W25-80 Models Sprung Mass Vertical Dynamic Response (Frequency Spectrum Analysis)

The dynamic responses of the models tend to cause a rotational dynamic response about the longitudinal axes, which

International Journal of Engineering Research & Technology (IJERT)
ISSN: 2278-0181
Vol. 12 Issue 07, July-2023

contributes to a downward shift of the COM. In Figure 8, the frequency domain analysis showed that the AIw25-80 model had a single dominant response signal with a frequency slightly lower than the other models. This can be explained by the destructive response of the sprung and unsprung mass, as well as the dominant vertical motions of the sprung mass within a relatively short interaction time frame.

Figure 9 and 10 depict the results of an analysis conducted on the E load configure model using the same kinematic excitations. The analysis also considered the effect of increasing the pothole depth to 50 mm while maintaining a constant vehicle speed of 60 km/h.

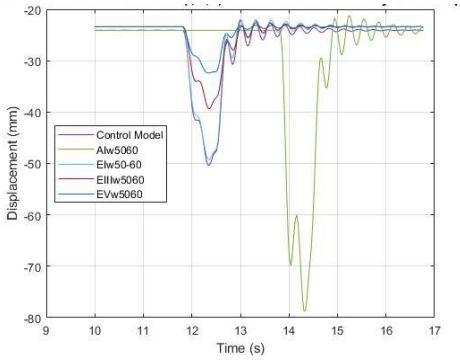

Figure 9: Control Model Versus AIw50-60 Versus E(I, III and V)W50-60 Models Sprung Mass Vertical Dynamic Response (Time Domain)

In Figure 9, the vertical dynamic motion responses of the system are shown in the time domain. The amplitudes of the sprung mass vertical displacement dynamic responses are lower than those of the AIw50-60, and they are not significantly different from the control model's sprung mass vertical dynamic response. Additionally, the same effects of COM downward shifts due to potholes encountered by the wheels are observed, regardless of changes in pothole depths.

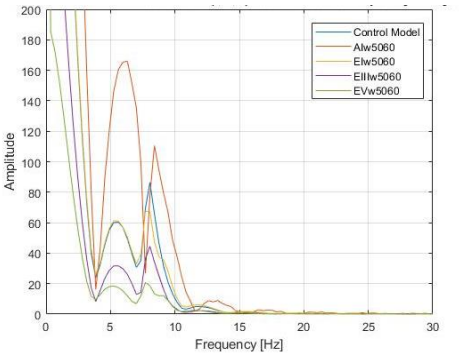

Figure 10: Control Model Versus AIw50-60 Versus E(I, III and V)W50-60 Models Sprung Mass Vertical Dynamic Response (Frequency Spectrum Analysis)

The reason for the reduction in the sprung mass dynamic response amplitudes in the E load configured models could be attributed to the concentration of the payload masses and its impact on the distribution of dynamic loads to the leaf springs and wheels. This is because the E load configured models introduce additional modes of dynamic responses such as rotational dynamic responses about the longitudinal and transverse axis, as they oscillate in the vertical axis (y-axis). As a result, the E load configuration tends to significantly offload the front axle, which may explain why it exhibits a low signal response amplitude at a frequency of around 11.9 Hz compared to the rear axle, as shown in Figure 10. Regardless of the loading configurations, high signal response amplitudes are observed for the symmetrical kinematic excitations. This can be explained by the fact that increasing pothole depth tends to increase the amplitudes of responses for the symmetrically loaded models.

In general, it can be argued that the dynamic response of the sprung masses is mainly governed by the kinematic excitation applied to the wheels, regardless of the loading configuration. This is evident from Figures 5, 7, and 9, where the symmetrically loaded models exhibit a high dynamic vertical displacement of the COM from its static equilibrium position, with further downwards displacement observed when the wheels are at the bottom of the pothole at all vehicle speeds and pothole depths. Similar vertical dynamic responses are observed for other models subjected to similar kinematic excitations. However, the control model (AIw25-60) is mainly influenced by the concentration of the load in the center, causing a dominant vertical displacement that further displaces the COM of the spindles downwards, compared to other models affected by a combination of sprung mass orientations and vertical displacements.

The models that were excited with V kinematics showed lower vertical dynamic displacements compared to the ones that were symmetrically loaded or excited on the rear wheels only. The V kinematics excitation introduces orientations on the tandem beams as the wheels lower into the potholes, inducing orientations onto the sprung mass through the front and rear axles, resulting in reduced unsprung mass vertical displacements. In the case of the E loaded model, these orientations seem to destructively interfere with the governing orientations of the chassis due to the load distribution. Therefore, the dominant harmonic motion observed on the V kinematically excited models could only be due to the vertical dynamic responses of the COM. The combined orientation about both the transverse and longitudinal axes could influence the system's dynamic responses to have relatively highly damped motions due to the load distribution. Therefore, it can be argued that the load configuration only affects the nature of the harmonic response and has minimal influence on the COM vertical displacement. The kinematic excitation seems to constructively interfere with the inertia effect of the sprung masses.

To examine the impact of a higher heavy vehicle speed, the same vehicle models were tested using a pothole depth of 25 mm and a heavy vehicle speed of 80 km/h. In general, the results for both models showed no significant difference when compared to the results obtained for the A(I,III,V)w25-60, B(I,III,V)w25-60, and E(I,III,V)w25-60 models in terms of the dynamic response of the COM vertical displacement. This could be explained by the reduced duration of the tire-pothole interactions, which may have shortened the response time of the sprung mass to the pothole interactions. However, a slight increase in their response amplitude can be observed. The findings suggest that increasing the heavy vehicle speed by 20 km/h does not seem to have a considerable effect on the nature of the vertical harmonic responses of these vehicle models, when compared to the control model's dynamic response of the COM vertical displacement of the sprung mass.

An analysis was conducted to investigate the impact of an increase in pothole depth on the vertical displacement dynamic

International Journal of Engineering Research & Technology (IJERT)
ISSN: 2278-0181
Vol. 12 Issue 07, July-2023

response of a heavy vehicle model under similar kinematic excitations and loading configurations. The results showed a slight increase in both the duration of tire-pothole interaction and amplitude of the oscillation responses. This finding is consistent with the literature by Turakhia and Modi (2016), which states that increasing the mass of a system can lead to noticeable increases in the oscillations of both the sprung and unsprung masses.

V. CONCLUSION AND RECOMMENDATIONS

The study introduced an a model capable of predicting the vertical dynamic response of heavy vehicles under general asymmetric loading and eccentric kinematic excitations. The study further investigated the effects of general asymmetries on the vertical vibration of the heavy vehicle's sprung mass. Based on the analysis and discussion of the results presented, it can be concluded that:

- The distribution of loads on the sprung mass affects the position of the COM along the vertical, transverse, and longitudinal axes, resulting in changes in the dynamic response of the heavy vehicle.
- Asymmetric loading configurations can cause significant static orientation of the sprung mass about the longitudinal and transverse axes.
- Inertia has a significant effect on the vertical dynamic response of the heavy vehicle's chassis, even in the presence of destructive interference responses of the suspensions.
- In conditions of symmetrical excitations, symmetrical heavy vehicle loading only has a dominant influence on the vertical COM dynamic displacement response.
- The nature of the chassis dynamic response is governed by the eccentric kinematic excitation exerted on the vehicle wheels.
- An increase in pothole depth and heavy vehicle speed amplifies and alters the nature of heavy vehicle dynamic responses to pavement profile interaction effects.

In future research, it is recommended to investigate the suspension system dynamics further to obtain precise dynamic responses of the sprung mass. This can be done by using a lumped axle assembly with a 3 or 2 Dimensional mass spring tire model to model the lumped mass spring damper suspension system more accurately. The effect of sprung mass inertia should also be studied in detail for symmetrical and asymmetrical loading configurations in the presence of large potholes and cases of overspeeding. Additionally, a mathematical 24 DOF model should be developed to validate these virtual model responses and examine the effects of general asymmetries on the vertical, lateral, longitudinal, and orientation dynamic responses of heavy vehicle models. Special attention should also be given to the unsprung mass to capture its dynamic influence on the connected tires. The developed model could provide insights into the effects of asymmetrical heavy vehicle loading on road infrastructures, which may be affected by various distress factors such as potholes and cracks of significant depths.

ACKNOWLEDGEMENTS

I would like to express my gratitude to the technical and support personnel in the Mechanical and Metallurgical Department at the University of Namibia for their assistance. Additionally, I extend my heartfelt thanks to my supervisors for their invaluable guidance in completing this project. It should be noted that this research was conducted as part of my master's program at the University of Namibia (UNAM).

REFERENCES

[1] F. Riccardo, L. Giovanni and F. J, "Numerical Modelling of Train Induced Vibrations," pp. 159-175, 2002.

[2] F. M. Soong, R. Ramli and A. Saifizul, "Between Simplicity and Accuracy: Effect of Adding Modelling detailes on quarter vehicle model accuracy," Advanced Computational and Applied Mechanics)ACAM) Resaerch Group, 2017.

[3] G. Bonin, G. Cantisani, G. Loprencipe and A. Ranzo, "Modelling od dynamic phenomena in road and iarport pavements," Dipartimento di Idraulica, Transporti e Strade (DITS)-Universita degli Studi di Roma, La Spienza, 2004.

[4] M. V, "OPTIMAL SUSPENSION DAMPING AND AXLE VIBRATION ABSORBER FOR REDUCTION OF DYNAMIC TIRE LOADS," Bell & Howell Information and Learning, Canada, 1998.

[5] N. F. Nangolo, "Analytical Extraction of Modal Parameters of Damped Mechanical Systems," International Multi-Topic Conference on Engineering and Science (IMCES), 2019.

[6] J. Soukup, J. Skočilas, B. Skočilasová and J. Dižo, "Vertical Vibration of Two Axle Railway Vehicle," Procedia Engineering, pp. 25-32, 2017.

[7] B. Simeon, C. F. Grupp and P. Rentrop, "A nonlinear Truck Model and Its Treatment as a Multibody System," Journal of Computation and Applied Mathematics, pp. 523-532, 1994.

[8] B. Mike and H. Damian, "Modelling and Assembly of the Full Vehicle: Modelling Leaf Springs," in THe Multibody Sysmtes Approach to Vehicle Dynamics (Second Edition), 2015.

[9] C. Guilherme, B. K. Mohammed and R. D. Renan, "Prediction of Aluminum Wheel Distortion under Pothole," ResearchGate: Science in the Age of Experience, 2016.

[10] N. Naveen, S. M. Yadav and A. S. Kumar, "A study on Potholes and Its Effects on Vehicular Traffic," International Journal of Creative Research Thoughts (IJCRT), pp. 258-263, 2018.